

SHEAR-WAVE SPLITTING OBSERVATIONS AND MEASUREMENTS AT THE GEOTHERMAL FIELD AT HENGILL, ICELAND

Chuanhai Tang *, Jose A. Rial *, Jonathan M. Lees *, and Maya Elkibbi **

* Department of Geological Sciences, University of North Carolina at Chapel Hill
Mitchell Hall, CB #3315, Chapel Hill, NC 27599, USA
e-mail: chhtang@email.unc.edu

** Department of Geology, American University of Beirut
P.O. Box: 11-0236/26, Beirut, Lebanon

ABSTRACT

During the summer of 2005 the seismicity at the Hengill geothermal field in Southwestern Iceland was recorded for forty-two days with an array of twenty-one PASSCAL L-28 4.5-Hz sensors. The array was divided into two parts, Eastern and Western, covering an area approximately 5 km in N-S by 10 km in E-W. During the deployment the array recorded approximately 4 microearthquakes on average per day at a sampling rate of 500 samples per second. Most seismicity has been observed to occur within the eastern part of the array. Epicenters of the earthquakes located in the east are highly clustered, while the focal depths are mostly shallower than 6 km, consistent with the estimate of the depth to the base of the brittle crust. Shear-wave splitting (SWS) was clearly observed in the seismic data from Hengill geothermal field. Measurements and consequent inversions of the shear-wave splitting parameters have provided evidence for a predominant crack system oriented approximately NNE-SSW, also consistent with the regional tectonics in Southwestern Iceland.

Keywords: shear-wave splitting, the Hengill geothermal field, stress-aligned crack, seismic imaging, fractured reservoir

INTRODUCTION

Iceland is situated on top of the Mid-Atlantic Ridge where the ridge interacts with the Iceland Hot Spot. Several volcanic centers, active and extinct, are located within the island. One of them is the Hengill volcanic center which lies on the plate boundary between the North America and the European crustal plates in Southwestern Iceland. The rifting of the two plates has opened a NNE trending system of normal faults with frequent magma intrusions. The Hengill central volcano and its transecting fissure swarm, extending 70–80 km long from the coast south of

Hengill to north of Lake Thingvallavatn with an associated graben structure, form the Hengill volcanic system. The Hengill central volcano is currently active and is the main volcanic production focus of the area associated with a high-temperature geothermal field. In Nesjavellir, in the northern part of the Hengill area, a 400 MW geothermal power plant has been in operation since 1987. Another active but less pronounced volcanic system, the Hrómundartindur volcanic system, lies at the eastern edge of the Hengill system, outside the Hengill fissure swarm. The area near Mount Hrómundartindur can be classified as the central volcano of this system; it is a separate focus of volcanic production with high geothermal activity.

During the months of July and August 2005, a 21-station, 3-component seismic array was deployed to the south of the Hengill central volcano, covering an area approximately 5 km in N-S by 10 km in E-W. The array was divided into two parts: the Western part including twelve stations numbering from H30 to H41, and the Eastern part with nine stations numbering from H70 to H78. The distribution of these stations is depicted in Figure 1. Also shown in Figure 1 are the epicenters of historical earthquakes occurring in this area between January 1995 and May 2005 which are retrieved from the online earthquake catalogues provided by the Icelandic Meteorological Office on a weekly basis in their web site (http://hraun.vedur.is/ja/viku/****/vika_#/hen.gif where **** are years and # are week numbers). Between July 2nd and August 12th the array continuously recorded the seismic activity in the study area for forty-two days. Each station in the seismic array consisted of a three-component short-period MARK4 L28 (4 Hz) seismic sensor, a data-logger or DAS (Data Acquisition System), a GPS antenna, and a 12V car battery. The data were collected continuously at a rate of 500 samples per second. The data recorded have been processed and analyzed to locate microearthquakes occurring in this area during the deployment and detailed analysis of

shear-wave splitting have been performed as will be presented in the following sections.

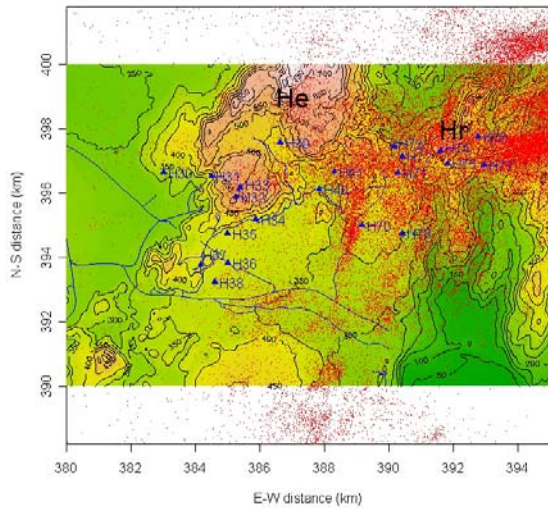


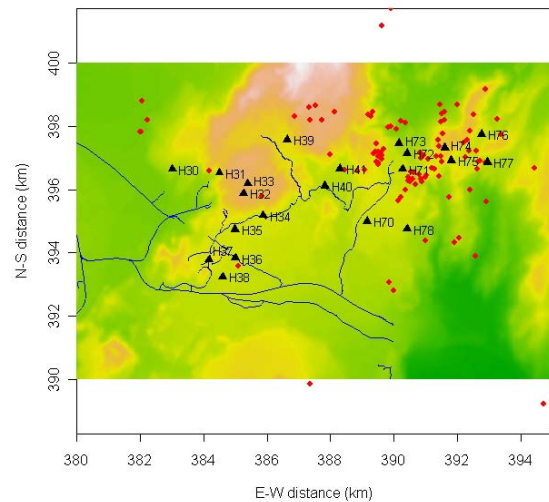
Figure 1. Distribution of the stations of PASSCAL seismic array in Hengill geothermal field, Iceland. The red points represent the locations of historical earthquakes from January 1995 to May 2005. 'He' is the Hengill central volcano and 'Hr' is the Mount Hrómundartindur.

SEISMICITY

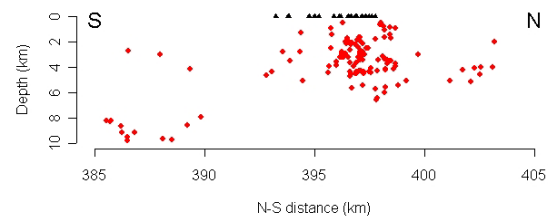
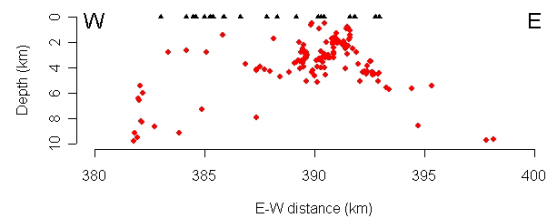
The variations in the daily number of seismic events detected by the array are shown in Figure 2. During the forty-two days of operation the array detected an average of 3 to 4 well-recorded events per day (observed at 5 or more stations). These are very small earthquakes with magnitudes probably no greater than 2. Figure 3a shows the epicenters of the earthquakes located within and in the vicinity of the array from July 5th to August 12th while Figure 3b shows the depth distribution of more earthquakes along E-W and N-S cross-sections respectively. The velocity model used in the locating program is from Tryggvason et al. (2002) and both P- and S-arrivals are used to provide sufficient constraints on the earthquake locations. It is apparent that most events occurred in the eastern part and were highly clustered around stations H71, H72 and H73. Essentially two clusters of events can be identified. Over 90 percent of the focal depths are shallower than 6 km, which is consistent with the estimate of the depth to the base of the brittle crust in this area (Tryggvason et al., 2002). Also note the gap of earthquakes between the depth range 6-10 km beneath the center of the Hrómundartindur volcanic system which agrees with the probable presence of a still-molten part of a mostly solidified magma chamber (Sigmundsson et al., 1997).



Figure 2. Daily number of events detected by the array throughout the deployment.



(a)



(b)

Figure 3. The seismicity recorded by the array from July 5th to August 12th is shown in (a). Totally 146 events are detected and 130 events properly located. The depth distribution of the events is shown in (b).

Shown in Figure 4 are focal mechanisms of the earthquakes indicated in Figure 3b. It can be found that the majority of them are strike-slip, normal-oblique strike-slip or oblique-normal events, although normal faulting is also common. All of these results are consistent with the regional tectonic settings.

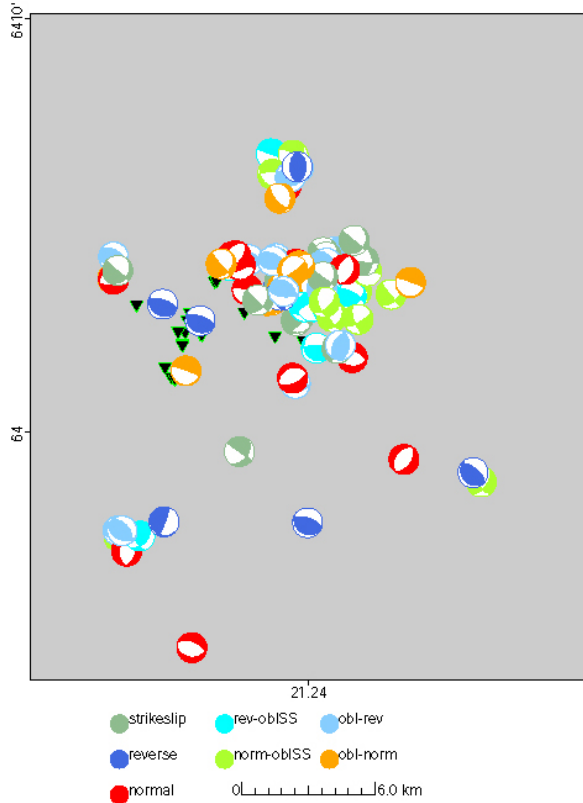


Figure 4. Focal mechanisms of the earthquakes shown in Figure 3b.

SHEAR-WAVE SPLITTING

Shear-wave splitting is an exploration method of proven reliability and unique imaging power. The method is based on the fact that a shear-wave propagating through rocks with stress-aligned micro-cracks will split into two waves, a fast one polarized parallel to the predominant crack direction, and a slow one polarized perpendicular to it (Crampin, 1981, 1984; Babuska and Cara, 1991). Two important parameters are associated with a shear-wave splitting event: the polarization direction of the fast shear wave (φ), and the differential time delay between the arrivals of the fast and slow shear waves (δt). Measuring the fast-shear wave polarization and time delay from local microearthquakes has become a valuable technique to detect the orientation and intensity of fracturing in the subsurface of fracture-controlled geothermal fields (e.g. Lou and Rial, 1997; Vlahovic et al., 2002a, 2002b; Elkibbi and Rial, 2003,

2005; Elkibbi et al., 2004, 2005; Yang et al., 2003, 2005; Rial et al., 2005; Tang et al., 2005a, 2005b).

Measuring the parameters

Shear-wave splitting is clearly recorded in the seismic data from Hengill geothermal area. In fact, we have recorded well developed splitting that clearly shows the prevalence of a dominate crack system oriented NNE-SSW in perfect agreement with the orientation of local fissure systems. An example of splitting in the data set is showed in Figure 5.

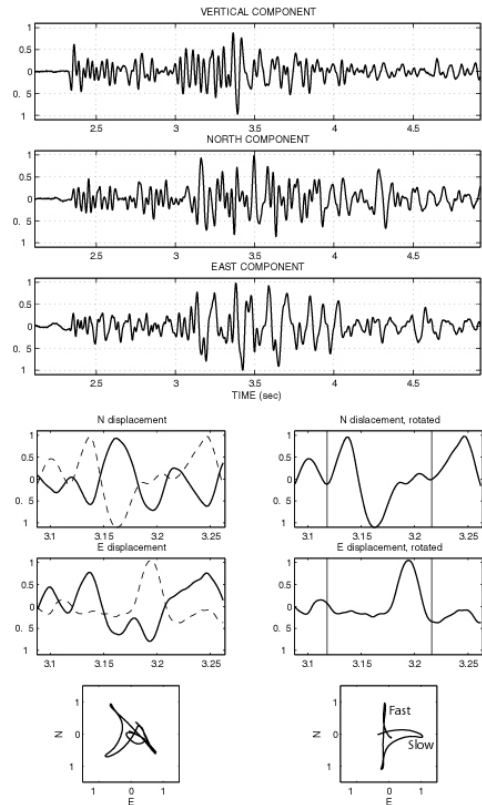


Figure 5. Example of shear-wave splitting. The event is identified as 200508060259 and recorded at H76. The amount of rotation is 134 degrees with a 56 ms time delay.

Fast shear-wave polarization angle φ is measured by interactive rotation of the seismogram until the horizontal particle motion plot shows that fast and slow shear-waves are oriented along the instrument's horizontal components (refer to the bottom half in Figure 5). The angle of rotation from the original polarization direction determines φ . Meanwhile the two shear-wave arrivals, which are often coupled in the original recording, separate out in time domain and δt can then be directly measured. In this study δt is normalized by dividing it by the length of the ray path in order to correctly compare delays from different paths.

So far the data from seven selected stations in the eastern part of the array (H70—H76) have been investigated to measure the fast shear-wave polarization and time delay. These stations are selected to ensure that most of the earthquakes fall into the shear-wave window, typically a right circular cone with vertex at the station and vertex angle equal to 35° , of the stations. Figure 6 shows the rose diagrams (polar histograms) of fast shear-wave polarization directions observed within the shear-wave window of the seven stations. It can be clearly seen from Figure 6 that the predominant polarization directions observed at stations H71, H72 and H75 are consistently pointing to a NNE-SSW orientation. H74 and H76 also display a major polarization in NNE-SSW, although there are still some cases showing an additional polarization perpendicular to the major direction, which is possibly due to the rough topography around these stations. H70 shows a similar but still worse pattern with two perpendicular polarization directions of almost equal strength, most probably accounted for by the fact that almost all the events within the shear-wave window of station H70 are far to the north (see also this station in Figure 7). Finally, H73 shows a completely different dominant direction of polarization in NWW-SEE which is perpendicular to the one displayed at H71, H72 and H75. This might suggest the existence of a conjugate fault system associated with the main NNE-SSW fissure system.

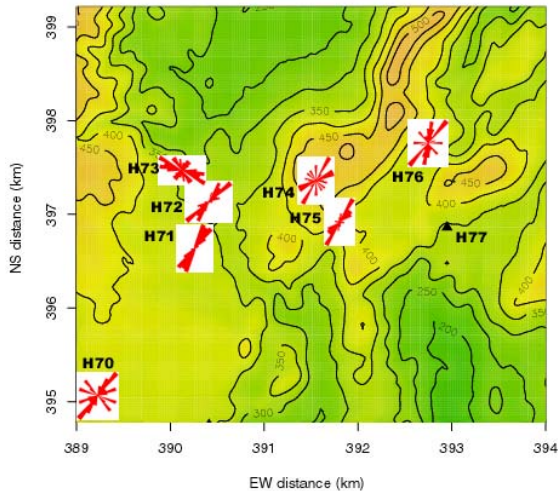


Figure 6. Rose diagrams showing the fast shear-wave polarization directions observed at the seven selected stations in the eastern part of the seismic array.

To inspect the azimuthal distribution of polarization angles, equal-area projection plots of the observed polarizations at all the seven selected stations are shown in Figure 7. For most of the stations, the shear-wave splitting events within the shear-wave

window come basically from all the four quadrants which can also be compared with the distribution of located epicenters in Figure 3a. The only exception is H70 where all associated earthquakes are projected on the northern hemisphere since it is far to the south of the earthquake clusters. Also note that at H72 the observed polarizations projected on the western hemisphere are in general slightly different from those on the eastern hemisphere although sharing the common NNE-SSW orientations, suggesting two unique sets of cracks with different strikes to the west and east of station H72 respectively.

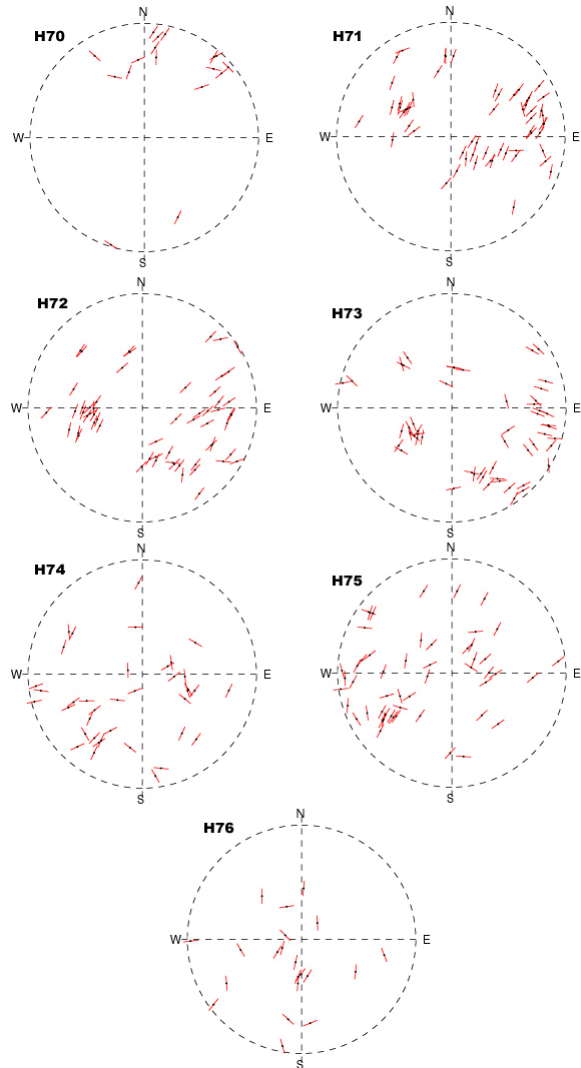


Figure 7. Observed fast shear-wave polarization directions at the seven stations plotted on the equal-area projection.

Inversion for crack geometry and intensity

We use an inversion scheme employing both shear-wave splitting parameters ϕ and δt (Yang et al., 2003, 2005). As has been extensively discussed in many

previous studies, ϕ mainly depends on the angle between the crack normal and the seismic ray while δt is proportional to the crack density along the ray path. Essentially, inversion efforts are expected to identify regions of different crack densities in Hengill geothermal field and to invert for 3-D fracture geometry in the subsurface. Based on seismic ray coverage and depending on the spatial patterns and azimuthal distributions of observed polarizations and time delays in the equal-area projection plots, crack-induced anisotropy in Hengill geothermal area is mainly modeled by a single system of vertical cracks, since most of the stations we have analyzed so far showed just one chief polarization direction (Figure 6). The recording of a single prevalent polarization may in general be accounted for by anisotropic effects due to parallel vertical cracks. In this case, the chief polarization orientation is parallel to the strike of the main crack system in the neighborhood of the station.

The inversion results for crack strike, crack dip, and crack density using the measured fast shear-wave polarization directions and differential time delays from the seven selected seismic stations in Hengill geothermal field are listed briefly in Table 1. The results at H71, H72, H75 and H76 are generally consistent with the assumption of the single set model in terms of their nearly vertical dipping angles and relatively low crack densities. The results of crack strikes are also in good agreement with the general NNE-SSW orientation of the fissure system. The crack strikes at H70 and H74 are more close to NEE-SWW and the dipping angles are more biased from vertical with a much higher crack density compared with the previous four sites. The results at H70 are even worse due to its far distance from the epicenters of the earthquakes. The inverted crack strike at H73 is roughly perpendicular to the dominant strikes of all other stations while the dipping angle is also somewhat biased from vertical.

Table 1. Inversion results for crack parameters in Hengill geothermal field.

Station ID	Crack Strike (Degree)	Crack Dip (Degree)	Crack Density
H70	72	-18	0.084
H71	27	89	0.048
H72	40	89	0.047
H73	-61	60	0.071
H74	54	63	0.077
H75	31	-87	0.043
H76	8	-89	0.033

CONCLUSIONS

A 21-station, 3-component digital seismic array was deployed near the Hengill geothermal field in Southwestern Iceland in July and August of 2005.

The seismic data set we have collected there is sampled at 500 sps which is high enough to allow detection of even the smallest variations in crack geometry and density. The seismicity in Hengill during the period of deployment of the array was not very high (3-4 usable events per day on average), with most epicenters clustered within the eastern part of the array. Over 90 percent of the focal depths are shallower than 6 km suggesting an approximate depth of 6 km to the base of brittle crust.

There is clear evidence of shear-wave splitting in the seismic data set. The observed prevalence of a crack system oriented in NNE-SSW, as well as the inverted crack strikes of most stations, is consistent with the anticipated direction of major fractures in the area. The only exception occurs at H73 where the observed main polarization direction and the inverted crack strike are approximately perpendicular to those of all other stations, which may indicate the existence of the conjugate of the main fracture system.

REFERENCES

- Babuska, V. and Cara, M. (1991), *Seismic Anisotropy in the Earth*, Modern Approaches in Geophysics, Vol. 10, pp. 217, Kluwer Academic Publishers, The Netherlands.
- Crampin, S. (1981), A review of wave motion in anisotropic and cracked elastic media, *Wave Motion*, 3, 343-391.
- Crampin, S. (1984), An introduction to wave propagation in anisotropic media, *Geophys. J. Roy. Astr. Soc.*, 76, 17-28.
- Elkibbi, M., and Rial, J.A. (2003), Shear-wave splitting: an efficient tool to detect 3D fracture patterns at The Geysers, California, *Proc. Geothermal Reservoir Engineering*, Stanford, 28, 143-149.
- Elkibbi, M., Yang, M., and Rial, J.A. (2004), Imaging crack systems in The Geysers with shear-wave splitting, *Geothermal Resources Council (GRC) Transactions*, 28, 789-800.
- Elkibbi, M., Yang, M., and Rial, J.A. (2005), Crack-induced anisotropy models in The Geysers geothermal field, *Geophys. J. Int.*, 162, 1036-1048.
- Elkibbi, M., and Rial, J.A. (2005), The Geysers geothermal field: results from shear-wave splitting analysis in a fractured reservoir, *Geophys. J. Int.*, 162, 1024-1035.

Lou, M., and Rial, J.A. (1997), Characterization of geothermal reservoir crack patterns using shear-wave splitting, *Geophysics*, 62, 487-495.

Rial, J.A., Elkibbi, M., and Yang, M. (2005), Shear-wave splitting as a tool for the characterization of geothermal fractured reservoirs: lessons learned, *Geothermics*, 34, 365-385.

Sigmundsson, F., Einarsson, P., Rognvaldsson, Th.S., Foulger, G.R., Hodgkinson, K.M., and Thorbergsson, G. (1997), The 1994-1995 seismicity and deformation at the Hengill triple junction, Iceland: Triggering of earthquakes by minor magma injection in a zone of horizontal shear stress, *J. Geophys. Res.*, 102:B7, 15151-15161.

Tang, C., Rial, J.A., Lees, J. M., and Thompson, E. (2005a), Seismic Imaging of the Geothermal Field at Krafla, Iceland, *Proc. Geothermal Reservoir Engineering*, Stanford, 30, 464-471.

Tang, C., J. A. Rial, and J. M. Lees (2005b), Shear-wave splitting: A diagnostic tool to monitor fluid pressure in geothermal fields, *Geophys. Res. Lett.*, 32, L21317, doi:10.1029/2005GL023551.

Tryggvason, A., Rognvaldsson, Th.S., and Flovenz, O.G. (2002), Three-dimensional imaging of the P- and S-wave velocity structure and earthquake locations beneath Southwest Iceland, *Geophys. J. Int.*, 151, 848-866.

Vlahovic, G., Elkibbi, M., and Rial, J.A. (2002a), Shear-wave splitting and reservoir crack characterization: the Coso geothermal field, *J. Volcanol. Geothermal Res.*, 120, 123-140.

Vlahovic, G., Elkibbi, M., and Rial, J.A. (2002b), Temporal variations of fracture directions and fracture densities in the Coso geothermal field from analyses of shear-wave splitting, *Proc. Geothermal Reservoir Engineering*, Stanford, 27, 415-421.

Yang, M., Elkibbi, M., and Rial, J.A. (2003), Modeling of 3D crack attributes and crack densities in geothermal reservoirs, *Proc. Geothermal Reservoir Engineering*, Stanford, 28, 321-327.

Yang, M., Elkibbi, M., and Rial, J.A. (2005), An inversion scheme to model subsurface fracture systems using shear wave splitting polarization and delay time observations simultaneously, *Geophys. J. Int.*, 160, 939-947.